The Journal of Clinical Pharmacology
2022, 62(1) 87–98

DOI: 10.1002/jcph.1950

Population Pharmacokinetics and Pharmacodynamics of Burosumab in Adult and Pediatric Patients With X-linked Hypophosphatemia

Sun Ku Lee, PhD[1], Nathalie H. Gosselin, PhD[2], Julie Taylor, PhD[1], Mary Scott Roberts, MD[1], Kathleen McKeever, PhD[1], and Jack Shi, PhD[1]

Abstract

Burosumab is a fully human monoclonal antibody against fibroblast growth factor 23, which has been approved to treat X-linked hypophosphatemia (XLH) in adult and pediatric patients. The present work describes the pharmacokinetics (PK) of burosumab and the pharmacokinetic-pharmacodynamic (PK-PD) relationship between burosumab and serum phosphorus in adult and pediatric patients with XLH. A total of 2844 measurable serum concentrations of burosumab and 6047 measurable serum concentrations of phosphorus in 277 subjects from 9 clinical studies were included in the population PK and PK-PD modeling. The serum concentration of burosumab following a subcutaneous administration was well described by a population PK model comprising a first-order absorption, 1-compartmental distribution, and a linear elimination. The relationship between serum burosumab and serum phosphorus was adequately described by a sigmoid maximal efficacy model. Body weight was the only covariate associated with PK and PK-PD parameters. No other intrinsic factors affected PK or PK-PD relationship in adult and pediatric patients with XLH. Further simulations helped to guide the dosing regimen of burosumab in adult and pediatric patients with XLH including age groups with no clinical data.

Keywords

burosumab, pharmacodynamics, pharmacokinetics, serum phosphorus, X-linked hypophosphatemia

X-linked hypophosphatemia (XLH) is a genetic disease inherited as an X-linked dominant trait and is characterized by the inadequate mineralization of bone leading to a spectrum of abnormalities such as rickets, osteomalacia, lower limb deformity, impaired growth, bone pain, and nontraumatic fractures/pseudofractures.[1,2] XLH is caused by loss-of-function mutations in a phosphate-regulating gene with homologies to endopeptidase located on the X chromosome (*PHEX*), which leads to elevated expression of fibroblast growth factor 23 (FGF23).[3] FGF23 reduces serum phosphorus levels by (1) inhibiting phosphate reabsorption in the renal proximal tubule and (2) by inhibiting 1-alpha hydroxylase activity in the kidney, which decreases serum 1,25-dihydroxyvitamin D [$1,25(OH)_2D$] levels and results in decreased phosphorus absorption from the gastrointestinal tract. Excess FGF23 leads to hypophosphatemia associated with abnormalities manifested in patients with XLH.[4]

Burosumab (Crysvita) is a fully human monoclonal antibody (immunoglobulin G_1 [IgG_1]) designed to bind and inhibit the biologic activity of elevated FGF23.[5] By blocking excess FGF23 in patients with XLH, burosumab increases phosphate reabsorption from the kidneys and the production of 1,25-dihydroxyvitamin D, which enhances intestinal absorption of phosphate and calcium.[6] In multiple clinical studies, burosumab increased serum phosphorus to the normal range and subsequently demonstrated clinical benefits such as the improvements in bone mineral metabolism, rickets, growth, and osteomalacia in pediatric XLH subjects and bone mineral metabolism, osteomalacia and fracture healing in adult subjects with XLH.[7–10] Based on the outcomes from these clinical studies, burosumab received marketing authorizations for the treatment of XLH in adult and pediatric patients 6 months of age and older.

Initially, the pharmacokinetics (PK) and pharmacodynamics (PD) of burosumab in adult subjects with

[1]Ultragenyx Pharmaceutical Inc., Novato, California, USA
[2]Certara Strategic Consulting, Princeton, New Jersey, USA

Submitted for publication 6 April 2021; accepted 3 August 2021.

Corresponding Author:
Sun Ku Lee, PhD, 5000 Marina Parkway, Brisbane, CA 94005, USA
Email: skulee@ultragenyx.com

XLH were characterized using the data from 3 clinical studies and reported previously.[11,12] Briefly, burosumab exhibited typical PK behaviors similar to other IgG_1 monoclonal antibodies (ie, slow absorption following a subcutaneous administration, low clearance, and long half-life). A sigmoid maximal efficacy (E_{max}) model adequately described the relationship between the serum burosumab concentrations and the serum phosphorus levels.

After the initial analyses, multiple clinical studies in adult and pediatric subjects with XLH were conducted, and additional data became available. Thus, we aimed to analyze the comprehensive PK and PD data in adult and pediatric subjects with XLH from a total of 9 clinical studies, including the 3 adult clinical studies used in the initial analyses.[11,12] The objectives of the current population PK and PK-PD analyses were to (1) characterize the PK of burosumab in adult and pediatric patients with XLH, (2) build PK-PD relationship to guide the effective and safe use of burosumab in adult and pediatric patients with XLH, and (3) investigate the impact of covariates on the PK of burosumab and the PK-PD relationship between burosumab and phosphorus levels in humans. The final PK and PK-PD models were used to determine the optimal dosing regimen in pediatric patient groups who had not participated in clinical studies.

Methods

Clinical Studies and Sample Collections

The PK and PD data were obtained from 6 clinical studies in 183 adult subjects with XLH and 3 clinical studies in 94 pediatric subjects (1-12 years of age) with XLH (NCT00830674, NCT01340482, NCT01571596, NCT02163577, NCT02750618, NCT02312687, NCT02526160, NCT02915705, and NCT02537431). The clinical study protocols were approved by relevant local institutional review boards or ethics committees at the investigative sites (Supplemental Information 1), and all patients provided written informed consent before enrollment. All studies were conducted in accordance with the US Code of Federal Regulations, Good Clinical Practice, 21 Code of Federal Regulations Parts 50, 56, and 312, the ethical principles set forth in the Declaration of Helsinki, the International Conference on Harmonization harmonized tripartite guideline regarding Good Clinical Practice and the ethical requirements referred to in the European Union directive 2001/20/EC.

Study participants received either a single dose or multiple doses of burosumab every 2 weeks or every 4 weeks. The dose levels of burosumab ranged from 0.05 to 1.2 mg/kg and intra-subject titration was allowed depending on the serum phosphorus levels and safety data. In the first single-ascending dose study, both intravenous and subcutaneous (SC) administration of burosumab were explored. However, only SC administration of burosumab was explored in the subsequent clinical studies. Thus, PK and PD data only from subjects following SC administrations of burosumab were included in the current analyses.

Blood samples were collected to measure serum burosumab (PK) and phosphorus (PD) at time points specified in the respective study protocols. The current analyses included 2844 measurable serum concentrations of burosumab (PK analysis) and 6047 measurable concentrations of serum phosphorus (PD analysis) from a total of 9 clinical studies in 277 subjects. The description of clinical studies and sample collections is provided in Supplemental Information 2.

Bioanalytical Methods

Serum samples were analyzed for burosumab using validated enzyme-linked immunosorbent assay or electrochemiluminescent (ECL) assays. For enzyme-linked immunosorbent assay, the lower limit of quantitation (LLOQ) was 50 ng/mL, with a linear range of 50 to 3000 ng/mL. For ECL assay, 2 independent analyzing laboratories validated the same methods but the LLOQ and linear range were slightly different. For the first ECL assay, LLOQ was 50 ng/mL, with a linear range of 50 to 10 000 ng/mL. For the second ECL assay, LLOQ was 36 ng/mL, with a linear range of 36 to 9500 ng/mL. All of these assays demonstrated consistent results by testing the same set of serum samples. Bioanalytical methods described in this section were reported in detail previously.[11]

Serum samples were analyzed for the presence of antidrug antibodies (ADAs) using a validated solid phase extraction and acid dissociation method. The drug tolerance of this assay is up to 80 μg/mL and the sensitivity/LLOQ is 54 ng/mL. Serum samples were analyzed for the total FGF23 using a validated ECL assay. LLOQ was 30 pg/mL, with a linear range of 30 to 12000 pg/mL. Serum phosphorus samples were analyzed as a part of standard clinical chemistry test panel using established Clinical Laboratory Improvement Amendments/College of American Pathologists (CLIA/CAP) accredited assays at CLIA/CAP certified central laboratories.

Handling of Data

Missing PK and PD data were excluded from the current analyses. Serum concentrations of burosumab below the lower limit of quantitation (BLQ) were excluded from the population PK analysis. Similarly, burosumab concentrations above the limit of quantification due to the failed quantitation after dilutions were excluded from the population PK analysis.

For pediatric patients, creatinine clearance (CR_{CL}) was derived using the Schwartz equation:

$$\text{1 week to} \leq \text{1 year old : CRCL}\left(\text{mL/min/1.73m}^2\right) = 0.45 \times \frac{HT}{CREAT} \quad (1)$$

$$\text{1 year to} \leq \text{12 years old : CRCL}\left(\text{mL/ min /1.73m}^2\right) = 0.55 \times \frac{HT}{CREAT} \quad (2)$$

where HT is height in centimeters and CREAT is serum creatinine in milligrams per deciliter.

For adult patients, CR_{CL} was derived using the Cockcroft and Gault equation:

$$\text{CRCL (mL/min)} = (140 - AGE) \times WT \times \frac{0.85\,(\textit{if female})}{72} \times CREAT \quad (3)$$

where CREAT is the serum creatinine in mg/dL, WT is the body weight in kg, and AGE is age in years.

Population PK Modeling

The structural PK model describing the concentration-time profiles was determined on the basis of the exploratory analyses and population PK modeling reported previously.[12] A 1-compartmental disposition model with the first-order absorption was selected as the structural model. Disposition PK parameters were allometrically scaled with time-varying body weights. Between-subject variability (BSV) was modeled with a log-normal distribution, and a combined error (ie, additive plus proportional error) model was selected to describe residual errors, as this model showed a statistically significant reduction in the objective function value (OFV) compared to the other models with only 1 error (ie, additive or proportional) term.

Model evaluation criteria included successful model convergence, reasonable parameter estimates with adequate precision, goodness-of-fit diagnostic plots, and other diagnostics such as shrinkage and simulation-based visual predictive checks (VPCs) where appropriate.[13]

Based on the graphical evaluation between covariates and PK parameters, the selected intrinsic factors were tested in the population PK model using the stepwise forward addition and backward elimination approach with a priori statistical significance criteria. The statistical significance level was 0.01 for the forward inclusion and 0.001 for the backward elimination, respectively, based chi-square distribution of OFV. The final model was then reassessed on the basis of other acceptance criteria including plausibility, model stability, and improvements in parameter precisions, relevant variance components, and diagnostic plots.

The performance of the final population PK models was evaluated with diagnostic plots and a prediction-corrected visual predictive check (pcVPC) plot. A pcVPC plot was conducted to ensure that simulation data from the final model could reproduce the observed data. Based on the estimates of the final model, concentration-time profiles of burosumab by age group were simulated using 1000 replicates of the patients in each group of stratification. The median and 90% prediction intervals of concentrations were computed and compared with the observed data within each bin and age group. Observed and simulated concentrations were corrected by typical population predictions within each bin.

Population PK-PD Modeling

In the clinical studies, serum phosphorus levels were measured more frequently than burosumab concentrations. To retain all observed serum phosphorus data and allow better characterization of the PK-PD relationship, observed serum phosphorus data in each subject were paired with time-matched burosumab concentrations simulated from the final population PK model. Individual PK parameters derived from the final population PK model and the actual dosing history were used to simulate burosumab concentrations at the PD collection time. Graphical evaluations showed that the change of serum phosphorus from baseline was correlated to the corresponding serum burosumab concentrations. The overall profile appeared to exhibit an increasing phase followed by a plateau. The range of burosumab concentration appeared to be sufficiently wide to estimate key model parameters. No distinct trends were observed between the adult and pediatric subjects with XLH. Based on these exploratory analyses, the PK-PD relationship was explored by applying multiple E_{max} models. BSV was modeled with a log-normal distribution as described in the population PK section. Multiple error models were evaluated, and a proportional error model best described the residual errors.

The evaluation of covariates on the PK-PD parameters followed the same approach applied in the population PK modeling. Based on the graphical evaluation between covariates and PK-PD parameters, the selected covariates were tested in the population PK-PD model using the stepwise forward addition and backward elimination approach similar to the population PK modeling.

The validation of the final PK-PD model was conducted by pcVPC on serum phosphorus. Based on the estimates of the final model, PK-PD profiles were simulated using 1000 replicates of the patients. Observed and simulated data were separated into

Table 1. Demographic Characteristics of Subjects With XLH

Demographic Characteristics	Infants (Age 1-2 y), N = 6	Children (Age 2-12 y), N = 88	Adults (Age >17 y), N = 183
Sex, n (%)			
Male	4 (67)	42 (48)	67 (37)
Female	2 (33)	46 (52)	116 (63)
Race/ethnicity, n (%)			
White	5 (83)	78 (89)	151 (83)
Black	0 (0)	3 (3)	5 (3)
Asian	1 (17)	1 (1)	25 (14)
Other	0 (0)	6 (7)	2 (1)
PHEX mutation, n (%)			
LPATH	1 (17)	7 (8)	119 (65)
PATH	4 (67)	75 (85)	21 (11)
VUS	1 (17)	4 (5)	18 (10)
Negative	0 (0)	0 (0)	10 (5)
Missing	0 (0)	2 (2)	15 (8)
Immunogenicity, n (%)			
Positive	1 (17)	12 (14)	11 (6)
Negative	5 (83)	76 (86)	172 (94)

LPATH, likely pathological mutation; PATH, pathological mutation; *PHEX*, phosphate-regulating gene with homologies to endopeptidase located on the X chromosome; VUS, variants of uncertain significance; XLH, X-linked hypophosphatemia.

disjoint bins within each age group. Medians and 90% prediction intervals of prediction-corrected concentrations were computed and visually compared with the prediction-corrected observed data within each age group.

PK-PD Simulations in Age Groups Without Clinical Data

Adolescents (12-17 years of age) and infants (< 1 year of age) were not enrolled in the pediatric XLH clinical studies. Prospective modeling and simulations were applied to select a dose regimen for these age populations. In adolescents, body weights with XLH were modeled using a General Additive Model for Location, Scale and Shape (GAMLSS) based on the actual baseline body weight distributions observed in pediatric (1 to <12 years old) and adult (18 to <69 years old) subjects included in the population PK and PK-PD analyses. Simulations of the GAMLSS model were then performed by randomly generating body weight values in adolescent XLH subjects from 12 to 17 years of age, inclusively. In infants, the PK and PK-PD time profiles at steady state were simulated using the model parameters from the final population PK and PK-PD models with virtual pediatric XLH patients. The range of body weights in infants (6-10 kg) was selected based on 5th and 95th percentile in the standard Centers for Disease Control and Prevention growth charts for healthy 6-month-old children. All simulation exercises were conducted with virtual pediatric patients including 1000 subjects within each age group.

Software

Nonlinear mixed-effect population PK and PK-PD modeling was performed using Phoenix NLME version 8 (Certara, Princeton, New Jersey). The exploration of data sets, and the generation of figures and tables were conducted using R version 3.5 with comprehensive R archive network and Certara Strategic Consulting packages. Model codes used for the population PK and PK-PD modeling are provided in Supplemental Information 3.

Results

Subject Characteristics

A total of 277 adult and pediatric subjects with XLH were included in the current analyses. The demographic and baseline characteristics of these subjects are provided in Table 1 and Table 2, respectively. Pediatric subjects were ≈34% of the total subjects included in the analyses. The majority of adult and pediatric subjects were White, and other races accounted for <20% of the overall subjects. Male and female subjects were almost evenly distributed in pediatric subjects with XLH, but female subjects were more prevalent among adult subjects with XLH. The baseline levels of bone-specific alkaline phosphatase, serum alkaline phosphatase, and FGF23, were ≈2- to 4-fold higher in pediatric subjects with XLH, compared to those in adult subjects with XLH. In general, these bone-related biomarkers are expected to be higher in pediatric subjects, as bones in the younger pediatric subjects grow rapidly over time.

Population PK Modeling

A total of 3177 PK samples were collected from 94 pediatric and 183 adult subjects with XLH who received SC doses of burosumab. Among those, 2844 measurable concentrations of burosumab were included in the population PK analysis of burosumab. Since 10.5% of

Table 2. Baseline Characteristics of Subjects With XLH

Baseline Characteristics	Mean (%CV)			Reference Range[g]
	Infants (Age 1-2 y), N = 6	Children (Age 2-12 y), N = 88	Adults (Age >17 y), N = 183	
Bone alkaline phosphatase (μg/L)	172 (59.6)[a]	161 (37.9)[b]	25 (67.8)[c]	Male: 4-21; female: 3-15 (premenopausal) Female: 4-23 (postmenopausal)
Serum albumin (g/dL)	4.60 (3.64)	4.46 (5.55)	4.33 (6.87)	3.5-5
Serum alkaline phosphatase (U/L)	564 (33.8)	482 (25.7)	122 (41.5)	50-120
Serum alanine aminotransferase (U/L)	18 (33.7)	16 (31.3)	25 (66.3)	10-40
Estimated creatinine clearance (mL/min in adults; mL/min/1.73 m^2 in children)	230 (52.5)	169 (21.4)[d]	146 (39.9)	75-125 (mL/min/1.73 m^2)
Serum intact FGF23 (pg/mL)	300 (33.1)[e]	326 (125)	142 (185)[f]	8-54
Serum phosphorus levels (mg/dL)	2.6 (12.7)	2.4 (13.4)	2.0 (17.6)	2.5-4.5

CV, coefficient of variation.
[a] n = 3;
[b] n = 62;
[c] n = 180;
[d] n = 86;
[e] n = 5;
[f] n = 166.
[g] Reference range was obtained from Zhang et al[12] and laboratory medicine. Unless specified, reference range indicates adults.

PK samples were BLQ, no alternate methods (eg, M3) were tested to evaluate the impact of removing BLQ and above the limit of quantification concentrations as suggested by Beal.[14] The number of BLQ and measurable samples for each age group is provided in Supplemental Information 4.

The best structural model describing the observed burosumab concentration data was the first-order absorption and 1-compartmental disposition with linear elimination model. PK parameters included the first-order rate of absorption without a lag time, apparent clearance (CL/F), and volume of distribution (V/F). CL/F and V/F were allometrically scaled with individuals' time-varying body weights (WTs). Time-varying WTs were used in the modeling to account for the rapid growth of pediatric patients over the treatment period. BSV of PK parameters was assessed using a log-normal distribution without correlation.

Based on the graphical evaluations, most covariates did not reveal clear trends; thus, further analyses were not conducted. Key covariates (age, ADAs, and FGF23) were further tested using a forward inclusion and backward elimination as described in the Methods section considering the observed trends or biological significance. A stepwise covariate showed that age (continuous variable) or age population (categorical variable, ie, adults vs children vs infants) was not a significant covariate to influence burosumab PK. Similarly, presence of positive ADAs showed no statistically significant effect on the PK parameters. Due to the significant increases in total FGF23 levels (free and bound to burosumab) after administration of burosumab, the potential covariate effect of time-varying total FGF23 concentrations was also assessed. A stepwise covariate analysis indicated that time-varying total FGF23 concentrations had no statistically significant effect on CL/F or V/F. Overall, no other intrinsic or extrinsic factors affected the absorption and disposition of burosumab after the time-varying WT had been allometrically scaled with CL/F and V/F. Therefore, the base model including allometric WT effects was selected as the final burosumab PK model. Diagnostic plots for covariate analyses are provided in Supplemental Information 5.

The final population PK parameters are presented in Table 3. The estimated first-order rate of absorption (0.395 1/day) indicates that burosumab is slowly absorbed following a subcutaneous administration. The CL/F and V/F for burosumab were 0.297 L/day and 9.02 L, respectively. These results suggest that burosumab is slowly cleared from the body with a limited volume of distribution. The model parameters were adequately optimized with acceptable precisions (relative standard error [RSE] from 6.39% to 25.5%). BSV for CL/F and V/F was 35.9 and 34.7%, respectively, indicating that the intersubject variability for these parameters are moderate.

The performance of the final population PK model was evaluated using standard diagnostic and VPC plots as presented in Figures 1 and 2, respectively. Overall, diagnostic plots indicate that the integrated population PK model adequately described the observed

Table 3. Final Population PK Parameters in Subjects With XLH

	PK Parameters (Unit)	Estimates (RSE, %)	BSV (Shrinkage, %)
Population mean parameters	K_a (1/day)	0.395 (7.89)	0% (FIX)
	V/F (L)	9.02 (13.9)	34.7% (24.3)
	CL/F (L/day)	0.297 (8.41)	35.9% (6.15)
Covariate effect of WT on CL/F	$(WT/70)^{exponent}$	0.912 (6.39)	
Covariate effect of WT on V/F	$(WT/70)^{exponent}$	1.05 (11.8)	
Residual errors	Additive error (ng/mL)	32.2 (17.7)	
	Proportional error (%)	20.7 (25.5)	

BSV, between-subject variability; CL/F, apparent clearance; K_a, first-order rate of absorption; PK, pharmacokinetic; RSE, relative standard error; V/F, apparent central volume of distribution; WT, body weight (kg); XLH, X-linked hypophosphatemia.
Effect of time-varying WT was centralized using 70 kg to facilitate the integration of adult data.

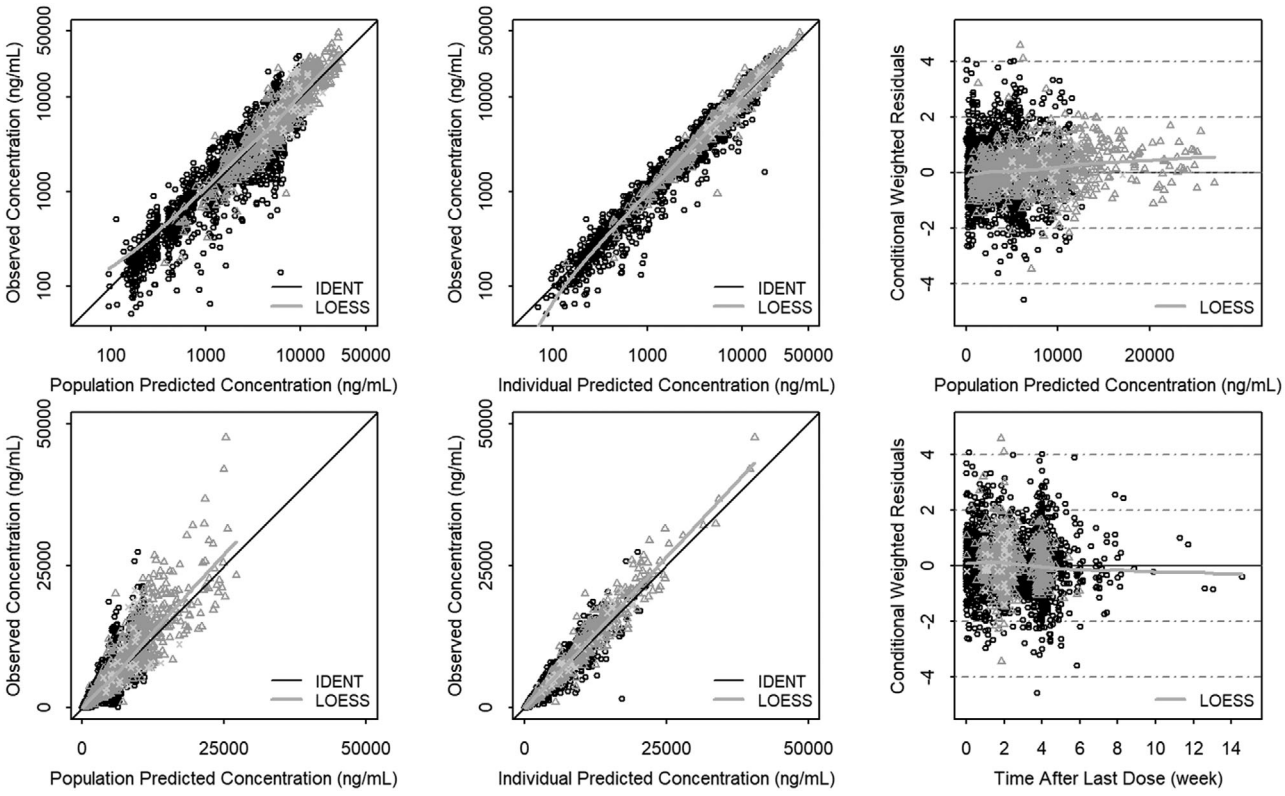

Figure 1. Diagnostic plots of the final Population PK model of burosumab in subjects with XLH. Light gray crosses = infants with XLH; gray triangles = children with XLH; black circles = adults with XLH. Observed concentrations versus individual and population predicted concentrations are presented on log scales in the upper left and upper central plots, and in linear scales in the lower left and lower central plots. Age categories are infants (1-2 years), children (2-12 years), and adults (>17 years). IDENT, line of identity; LOESS, locally weighted scatter plot smoothing; PK, pharmacokinetic; XLH, X-linked hypophosphatemia.

burosumab concentration-time profiles following the SC administrations at various dose levels and 2 dosing frequencies (every 2 weeks and every 4 weeks) in 277 adult and pediatric subjects with XLH. The VPC plots showed that the 90% prediction interval of predicted concentration-time profiles in the adult, child, and infant subjects mostly overlapped with the corresponding confidence intervals of observed concentrations at the respective 5th, 50th, and 95th percentiles. Due to the limited number of subjects in the infant group (N = 6), the predictive percentiles were associated with greater uncertainty for this age group.

Population PK-PD Modeling

The best structural model describing the PK-PD relationship was the sigmoidal E_{max} model including the response when no drug is present (E_0), half maximal effective concentration (EC_{50}), E_{max}, and γ, as well as BSV associated with model parameters. Based on the exploratory analyses, demographic factors (ie, sex,

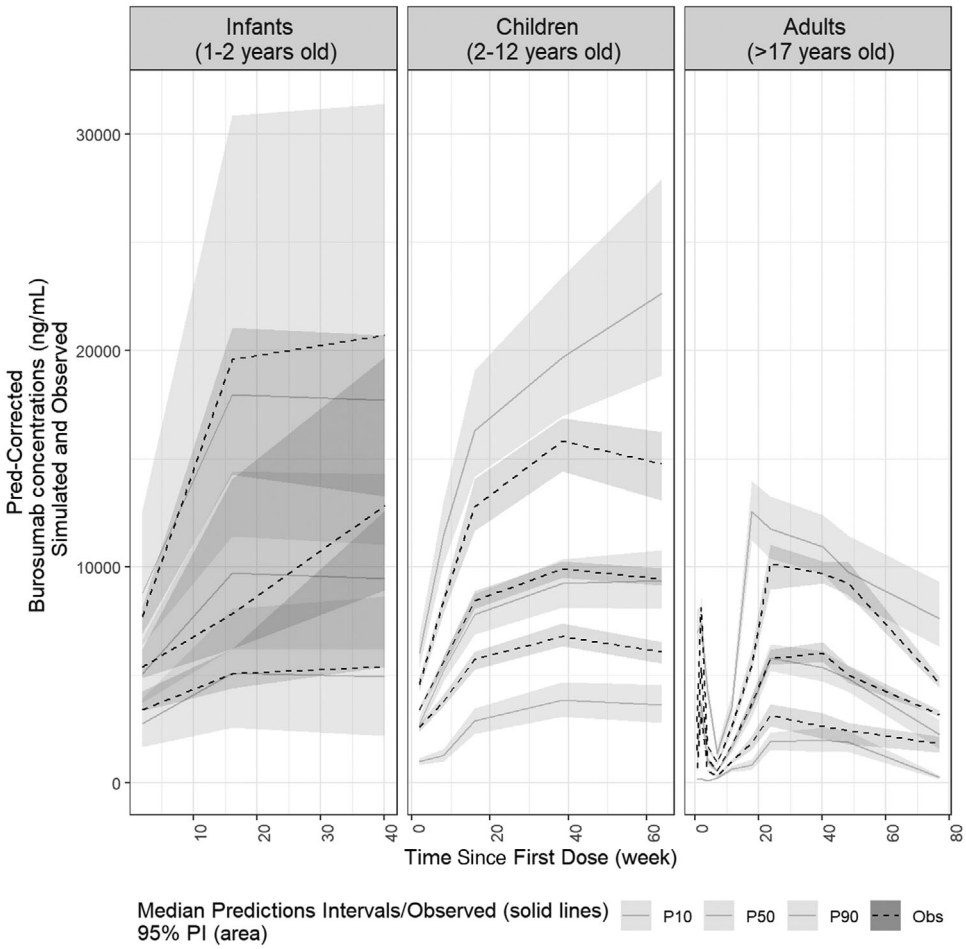

Figure 2. Prediction-corrected visual predictive check plots of the final population PK model of burosumab in subjects with XLH. Uncertainty on observations was determined by resampling the observations within each bin (N = 1000) and model predictions were based on 1000 replicates of the data set. Gray dashed lines represent percentiles of observed burosumab concentrations within each bin; gray shaded area represents 95th percentile interval of percentiles of predicted concentrations, and black shaded area represents 95th percentile interval of percentiles of observed concentrations. Obs, observations; P10, 10th percentile; P50, 50th percentile; P90, 90th percentile; PI, prediction interval; PK, pharmacokinetic; XLH, X-linked hypophosphatemia.

ethnicity, race, and country), baseline FGF23, and positive ADA did not appear to affect the model parameters. Thus, no further analyses were conducted for these covariates. A relevant trend was observed between individual random effects of model parameters (ie, E_0 and E_{max}) and intrinsic factors (ie, age and body weight). Consequently, the effects of age and WT on E_0 and E_{max} were tested using a formal covariate analysis as described in the Methods section. A stepwise covariate analysis indicated that WT and age showed significant effects on E_0 and E_{max}. However, the effect of age on the model parameters was not statistically significant after time-varying WT had been incorporated into E_0 and E_{max}. Considering the correlation between age and WT observed in the clinical studies, it was concluded that WT could describe the apparent effects of age on the model parameters. Therefore, the final PK-PD model was the sigmoidal E_{max} model incorporating WT onto E_{max} and E_0. Notably, the estimate of γ value was close to 1 (ie, 0.936) after the effects of WT were incorporated into the model. Thus, γ value was fixed to 1 to simplify the model.

The final PK-PD model parameters are provided in Table 4. BSV for model parameters ranged from 12% to 130%, indicating a wide range of subject variability. The model parameters were adequately optimized with acceptable precisions (RSE from 1.09% to 29.1%).

The diagnostic plots and VPC of the final PK-PD model are provided in Figures 3 and 4, respectively. Overall, the diagnostic plots indicate that the population PK-PD model adequately described the observed relationship between serum burosumab and phosphorus levels in adult and pediatric subjects with XLH. The VPC plots showed that the 90% prediction interval of predicted serum phosphorus in adult, children and infant subjects mostly overlapped with the corresponding

Table 4. Final Population PK-PD Parameters in Subjects With XLH

	PK-PD Parameters (Unit)	Estimates (RSE, %)	BSV (Shrinkage, %)
Population mean parameters	E_0 (mg/dL)	2.03 (1.09)	12.0% (11.7)
	EC_{50} (ng/mL)	4131 (13.3)	130% (28.3)
	Gamma	1 (FIX)	0 (FIX)
	E_{max} (mg/dL)	1.59 (5.49)	53.2% (36.6)
Covariate effect of WT on E_0	$(WT/70)^{exponent}$	–0.143 (8.83)	
Covariate effect of WT on E_{max}	$(WT/70)^{exponent}$	0.168 (29.1)	
Residual error	Proportional error (%)	13.2 (1.82)	

BSV, between-subject variability; E_0, response when no drug is present; E_{max}, maximal efficacy; EC_{50}, half maximal effective concentration; PD, pharmacodynamic; PK, pharmacokinetic; RSE, relative standard error; WT, body weight (kg); XLH, X-linked hypophosphatemia.
Effect of time-varying WT was centralized using 70 kg to facilitate the integration of adult data.

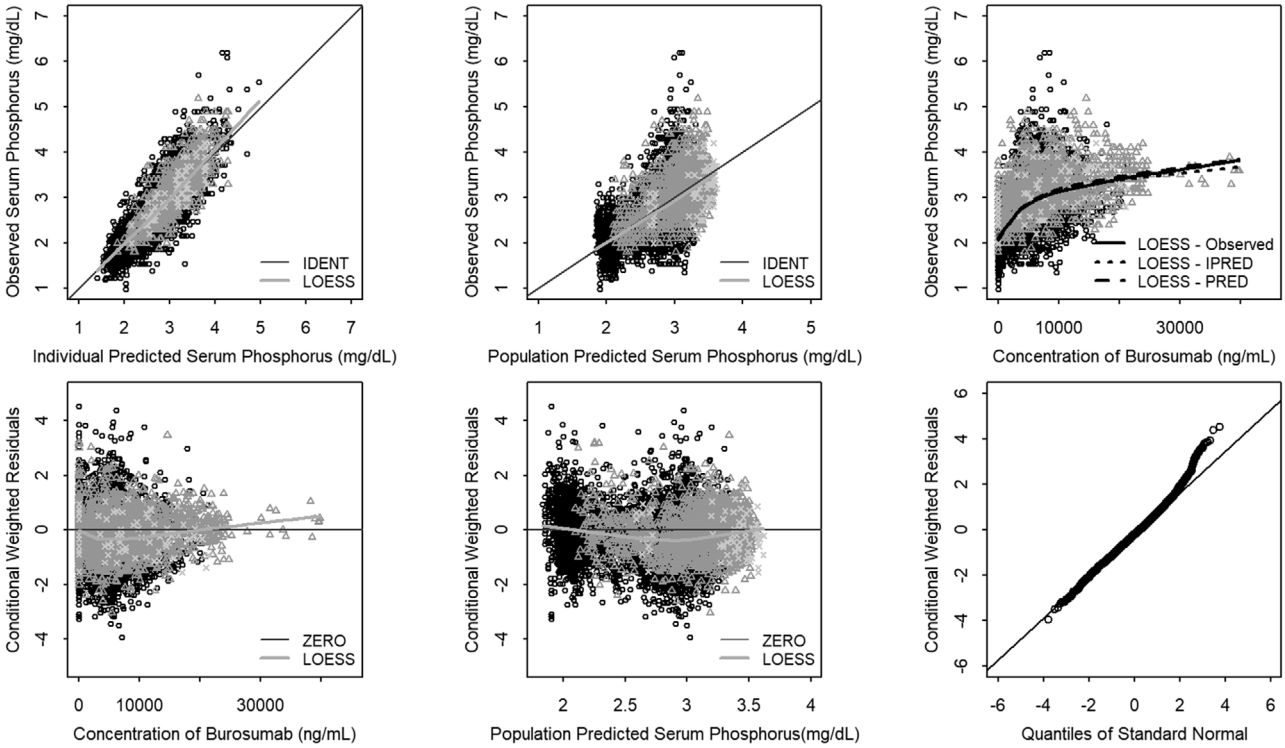

Figure 3. Diagnostic plots of the final population PK/PD model of serum phosphorus-burosumab relationship in subjects with XLH. Light gray crosses = infants with XLH; gray triangles = children with XLH; black circles = adults with XLH. Observed concentrations vs individual and population predicted concentrations are presented on log scales in the upper left and upper central plots, and in linear scales in the lower left and lower central plots. Age categories are infants (1-2 years), children (2-12 years), and adults (>17 years). IDENT, line of identity; LOESS, locally weighted scatter plot smoothing; PK, pharmacokinetic; XLH, X-linked hypophosphatemia.

confidence interval of observed serum phosphorus at the respective 5th, 50th, and 95th percentiles. Due to the limited number of subjects in the infant group (N = 6), the predictive percentiles were associated with greater uncertainty in this age group.

PK-PD Simulations in Age Groups Without Clinical Data

The final PK and PK-PD models were used to determine the dosing regimen for pediatric patient groups with XLH who had not participated in clinical studies. As indicated in the Methods section, prospective PK and PK-PD simulations were conducted in virtual populations of 2 age groups: adolescents (12-17 years of age) and infants (<1 year of age). In clinical studies, the dose levels of burosumab were escalated individually to reach the serum phosphorus to the normal range. Thus, the simulations were intended to determine the appropriate starting dosing regimen in the 2 patient groups. Based on the simulation results, the proposed starting dose regimens were 0.8 mg/kg every 2 weeks in pediatric patients weighing ≥10 kg and 1 mg/kg every 2 weeks in infants weighing <10 kg. As presented in Supplemental

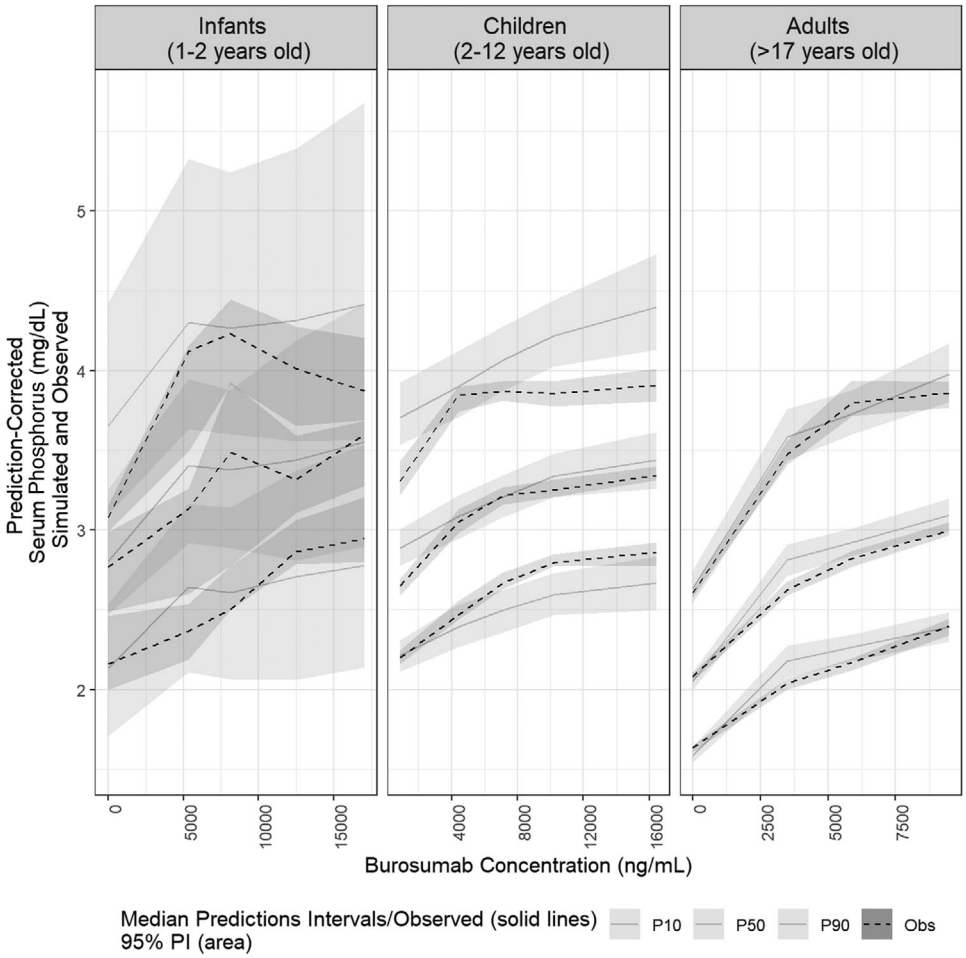

Figure 4. Prediction-corrected visual predictive check plots of the final population PK/PD model of serum phosphorus-burosumab relationship in subjects with XLH. Uncertainty on observations was determined by resampling the observations within each bin (N = 1000) and model predictions were based on 1000 replicates of the data set. Gray dashed lines represent percentiles of observed serum phosphorus levels within each bin; gray shaded area represents 95th percentile interval of percentiles of predicted levels, and black shaded area represents 95th percentile interval of percentiles of observed levels. Obs, observations; P10, 10th percentile; P50, 50th percentile; P90, 90th percentile; PD, pharmacodynamic; PK, pharmacokinetic; PI, prediction interval; XLH, X-linked hypophosphatemia.

Information 6, the projected mean serum phosphorus levels reached the normal range and peak serum phosphorus levels did not exceed the normal range (3.2-6.5 mg/dL) in the adolescent patients with XLH, at a dose of 0.8 mg/kg every 2 weeks. In infants with XLH, the projected serum phosphorus concentrations were within the normal phosphorus range at 1 mg/kg every 2 weeks, and these levels in infants appear to be similar to those in younger pediatric patients (1-5 years of age) at 0.8 mg/kg every 2 weeks (Supplemental Information 7). These results indicate that the proposed starting dose regimens were appropriate to achieve serum phosphorus levels within the normal ranges in these 2 pediatric age groups. Additional simulation results showing longitudinal changes of serum phosphorus by dose escalation in pediatric and adult patients are provided in Supplemental Information 8.

Discussion

Population PK and PK-PD analyses showed that the serum concentration-time profiles of burosumab were well described by a population PK model comprising a first-order absorption, 1-compartmental distribution and a linear elimination. The relationship between serum burosumab and serum phosphorus was adequately described by a sigmoid E_{max} model incorporating E_0, E_{max}, EC_{50}, and γ.

The PK parameters from the population PK model suggest that burosumab exhibited PK characteristics in common with typical monoclonal antibody therapeutics (ie, slow absorption, low clearance, small volume of distribution, and long half-life).[15,16] These results were consistent with the population PK analyses of burosumab previously reported using 3 clinical studies.[12] The model-estimated typical value of elimination

half-life in adult and pediatric patients with XLH ranged from 16 to 19 days, comparable to those reported for approved monoclonal antibodies with an IgG1 subtype.[16] Differences in the half-life between adult and pediatric subjects with XLH were small, indicating that the estimated half-life was not sensitive to body weight. This would support the weight-adjusted dosing regimen irrespective of age groups. No other intrinsic or extrinsic factors were identified to affect the PK of burosumab after the time-varying body weight had been allometrically scaled with CL/F and V/F.

As a monoclonal antibody, the exposure of burosumab may not be affected by renal impairment. However, renal impairment may be able to induce abnormal mineral metabolism leading to hyperphosphatemia. Therefore, burosumab is not recommended for patients with severe renal impairment. The model-estimated allometric exponents for CL/F and V/F in relation to body weight were 0.912 and 1.05, respectively. These results are consistent with other monoclonal antibodies reported in the literature, and it appears that burosumab follows similar PK profiles with typical monoclonal antibodies.[16] These results also support the weight-adjusted dosing regimen as similar exposure to burosumab is expected in patients with XLH irrespective of the range of body weights. The simulation results comparing the exposure of burosumab and corresponding serum phosphorus at steady state following a weight-adjusted dose (1 mg/kg every 4 weeks) and a fixed dose (70 mg every 4 weeks) indicate that the exposure of burosumab and serum phosphorus in adults following a weight-adjusted dose are similar to those in adults following a fixed dose (Supplemental Information 9). However, it appears that the BSV for burosumab exposure is smaller in subjects following a weight-adjusted dose than subjects following a fixed dose. Overall, these results support the recommendation to administer burosumab as a body weight–adjusted dose.

It should be noted that the effects of circulating FGF23 and positive immunogenicity on the PK of burosumab were evaluated with special attention to the mechanism of action of burosumab or the common effects of immunogenicity on the PK and PD of monoclonal antibody therapeutics.[17,18] As a fully human monoclonal antibody, the incidence of positive immunogenicity of burosumab was low in subjects with XLH (≈7%), and the positive immunogenicity did not affect the PK of burosumab. These findings are consistent with other fully human monoclonal antibodies.[15,16] The concentration levels of burosumab appear to be high to completely bind to the circulating FGF23 at dose levels tested in the clinical studies. Consistent with these observations, baseline FGF23 did not affect the PK of burosumab, indicating that the linear PK is consistent with expectations for monoclonal antibodies targeting against a soluble ligand such that the risk for target-mediated drug disposition would be low. This result is also consistent with baseline FGF23 not impacting drug clearance.[19] Overall, the lack of these covariate effects on the exposure of burosumab supports that dose adjustments are not required for these intrinsic factors.

Mechanistically, the temporal delay between burosumab concentrations and the changes of serum phosphorus from baseline could be feasible, as the neutralization of FGF23 by burosumab would precede the change of serum phosphorus levels. Usually, a hysteresis loop is observed to reflect the temporal delay between PK and PD data.[20] However, no hysteresis reflecting the temporal delay was observed between burosumab concentrations and the change of serum phosphorus from baseline following the SC administration of burosumab. Therefore, indirect or delayed PK-PD models accounting for the temporal delay were not explored in the current analyses. The sigmoidal E_{max} model appeared to describe the overall PK-PD relationship without time-dependent changes in the model parameters. Similar to the population PK model, the model parameters (ie, E_0 and E_{max}) for the population PK-PD model were dependent on subject's body weight. No other covariates affected the PK-PD relationship. The typical value of EC_{50} was 4131 ng/mL and time-invariant, suggesting an absence of pharmacodynamic changes over time following repeat dosing of burosumab. The current PK-PD model adequately described the observed data in both adult and pediatric subjects with XLH.

Body weight is the covariate for E_{max} and E_0. The effects of body weight on these parameters are likely due to different baseline levels of serum phosphorus and PD effects of burosumab between adult and pediatric patients. As serum phosphorus is important in the growth of bone in pediatric patients, baseline serum phosphorus tends to be higher in younger pediatric patients. Additionally, the maximum PD effects of burosumab appear to be greater in adult patients than pediatric patients. Body weights in pediatric patients are lower than adult patients, resulting in the significant effects of body weight on PK-PD parameters.

The BSV for E_0 and E_{max} (12% and 53%) were low to moderate, which may reflect the anticipated subject variability for baseline serum phosphorus and the maximum effect of burosumab on the increase of serum phosphorus. The BSV for EC_{50} was >100%, suggesting that the binding of burosumab to FGF23 may not lead to an unvaried pharmacological response. The high BSV for EC_{50} is partly due to the wide range of baseline FGF23 observed in clinical studies. This result supports the recommendation that the dose escalation

of burosumab should be individualized based on the level of serum phosphorus to achieve the maximum clinical benefit.

Serum phosphorus levels need to be maintained within the normal range because both hypophosphatemia and hyperphosphatemia can result in serious pathological effects.[21] In patients with XLH, burosumab is administered to increase the serum phosphorus up to the normal range but should not be increased beyond the upper limit of the normal range to prevent hyperphosphatemia. Therefore, the dose levels of burosumab were escalated individually to achieve serum phosphorus in the normal range in the clinical studies. Further dose adjustment was determined on the basis of the observed safety data and serum phosphorus levels. Considering the relatively tight range of normal serum phosphorus, the characterization of the PK-PD relationship is critically important to guide the optimal dosing regimen in patients with XLH. The population PK and PK-PD analyses helped to characterize the relationship between burosumab and serum phosphorus and subsequently guide the optimal dosing regimen to maintain the serum phosphorus within the normal range.

As body weight was the only relevant covariate to describe the subject variability in the PK of burosumab and the PK-PD relationship, the age of the patient population did not affect the dose selection of burosumab in pediatric patients with XLH. The changes in serum phosphorus from baseline were comparable between adult and pediatric subjects with XLH at the same body weight-adjusted dosing regimen. These results indicate that the same strategy to escalate and adjust dose levels based on the serum phosphorus levels and safety findings can be applied to both adult and pediatric patients with XLH.

Current model-based analyses were used to justify the dosing regimen in age groups that had not been included in the clinical studies (ie, <1 year of age, and 12-17 years of age). Infants (<1 year of age) were not included in the clinical studies mostly due to difficulties in recruiting patients in this age group. Adolescents (12-17 years of age) were not included in the clinical studies to minimize the bias in evaluating clinical assessments associated with rickets. Skeletal features in pediatric patients with XLH can be assessed adequately while the growth plates remain open. It is likely that the growth plates in adolescents would close during the study treatment period and not allow for rickets assessments. Despite the lack of clinical data in these age groups, the appropriate dosing regimen was proposed on the basis of the extrapolation of PK and PD using the current population PK and PK-PD models accounting for the appropriate range of body weights in the respective age groups. Simulation results suggest that the same body weight–adjusted starting dose across pediatric age groups is acceptable without adjusting dosing regimen for any other intrinsic or extrinsic factors. Notably, the risks of hyperphosphatemia were predicted to be very low in pediatric patients, alleviating the concern to escalate dose levels matched with the highest dose in adult patients with XLH. As indicated in Supplemental Information 8, simulation results indicated that the proportion of virtual pediatric patients reaching normal levels of serum phosphorus at trough increased from 12.7% to 67.0% when burosumab dose escalated from 0.3 mg/kg up to 2.0 mg/kg every 2 weeks. The proportion of virtual pediatric patients reaching normal serum phosphorus was ≈36% when virtual pediatric subjects received 0.8 mg/kg every 2 weeks. This dosing regimen was deemed appropriate as a starting dose in pediatric patients because an adequate number of patients appeared to reach normal serum phosphorus levels without increasing risks of hyperphosphatemia. The selection of an optimal dosing regimen in pediatric patients based on model-based extrapolation has been previously reported.[22] The FDA accepted the proposed dosing regimen based on the current model-based extrapolation and approved the use of burosumab in pediatric age groups that had not been included in the clinical studies.

Conclusion

Population PK and PK-PD analyses adequately characterized the PK of burosumab and PK-PD relationship between burosumab and phosphorus in adult and pediatric patients with XLH. Body weight was the only covariate associated with PK and PK-PD parameters. Model-based analyses helped to guide the dosing regimen of burosumab in adult and pediatric patients with XLH. Particularly, the model-based PK and PK-PD simulations support the use of burosumab in pediatric age groups (<1 year of age and 12-17 years of age) that were not included in clinical studies.

Acknowledgments

These studies were supported by Ultragenyx Pharmaceutical Inc. in partnership with Kyowa Kirin Co., Ltd. The authors thank Wendy Putnam for her insights on revising the manuscript.

Third-party writing assistance was provided by Kariena Dill, PhD, and paid for by Ultragenyx.

Conflict of Interest

S.L., J.T., and K.M. are current employees of Ultragenyx. J.S. and M.S.R. are former Ultragenyx employees and were employed at Ultragenyx Pharmaceuticals Inc. when these studies were conducted. N.H.G. is an employee of Certara and does not have any conflicts of interest to declare.

Data Availability Statement

The study protocol and statistical analysis plan for the studies mentioned in this manuscript will be available per regulatory requirement on the clinical trial registry website ClinicalTrials.gov with the tabulated results. For more details about the Ultragenyx data sharing commitment, please visit https://www.ultragenyx.com/pipeline/clinical-trial-transparency/

Funding

The studies described here were sponsored and funded by Ultragenyx Pharmaceuticals Inc. in partnership with Kyowa Kirin International plc.

References

1. Holm I, Econs M, Carpenter T. Familial hypophosphatemia and related disorders. In: FH G, H J, eds. *Pediatric Bone: Biology & Diseases*. 2nd ed. San Diego, CA: Elsevier; 2012:699-726.
2. Burnett CH, Dent CE, Harper C, Warland BJ. Vitamin D-resistant rickets Analysis of twenty-four pedigrees with hereditary and sporadic cases. *Am J Medicine*. 1964;36(2):222-232.
3. Carpenter TO. New perspectives on the biology and treatment of X-linked hypophosphatemic rickets. *Pediatr Clin N Am*. 1997;44(2):443-466.
4. Razzaque MS, Lanske B. The emerging role of the fibroblast growth factor-23–klotho axis in renal regulation of phosphate homeostasis. *J Endocrinol*. 2007;194(1):1-10.
5. Yamazaki Y, Tamada T, Kasai N, et al. Anti-FGF23 neutralizing antibodies show the physiological role and structural features of FGF23. *J Bone Miner Res*. 2008;23(9):1509-1518.
6. Fukumoto S. Physiological regulation and disorders of phosphate metabolism -pivotal role of fibroblast growth factor 23-. *Internal Med*. 2008;47(5):337-343.
7. Carpenter TO, Imel EA, Ruppe MD, et al. Randomized trial of the anti-FGF23 antibody KRN23 in X-linked hypophosphatemia. *J Clin Invest*. 2014;124(4):1587-1597.
8. Imel EA, Zhang X, Ruppe MD, et al. Prolonged correction of serum phosphorus in adults with X-linked hypophosphatemia using monthly doses of KRN23. *J Clin Endocrinol Metabolism*. 2015;100(7):2565-2573.
9. Carpenter TO, Whyte MP, Imel EA, et al. Burosumab therapy in children with X-linked hypophosphatemia. *New Engl J Med*. 2018;378(21):1987-1998.
10. Insogna KL, Briot K, Imel EA, et al. A randomized, double-blind, placebo-controlled, phase 3 trial evaluating the efficacy of burosumab, an anti-FGF23 antibody, in adults with X-linked hypophosphatemia: week 24 primary analysis. *J Bone Miner Res*. 2018;33(8):1383-1393.
11. Zhang X, Imel EA, Ruppe MD, et al. Pharmacokinetics and pharmacodynamics of a human monoclonal anti-FGF23 antibody (KRN23) in the first multiple ascending-dose trial treating adults with X-linked hypophosphatemia. *J Clin Pharmacol*. 2016;56(2):176-185.
12. Zhang X, Peyret T, Gosselin NH, Marier JF, Imel EA, Carpenter TO. Population pharmacokinetic and pharmacodynamic analyses from a 4-month intradose escalation and its subsequent 12-month dose titration studies for a human monoclonal anti-FGF23 antibody (KRN23) in adults with X-linked hypophosphatemia. *J Clin Pharmacol*. 2016;56(4):429-438.
13. Karlsson MO, Savic RM. Diagnosing model diagnostics. *Clin Pharmacol Ther*. 2007;82(1):17-20.
14. Beal SL. Ways to fit a PK model with some data below the quantification limit. *J Pharmacokinet Phar*. 2001;28(5):481-504.
15. Dirks NL, Meibohm B. Population pharmacokinetics of therapeutic monoclonal antibodies. *Clin Pharmacokinet*. 2010;49(10):633-659.
16. Ryman JT, Meibohm B. Pharmacokinetics of monoclonal antibodies. *Cpt Pharmacometrics Syst Pharmacol*. 2017;6(9):576-588.
17. Imel EA, Econs MJ. Fibroblast growth factor 23: roles in health and disease. *J Am Soc Nephrol*. 2005;16(9):2565-2575.
18. Dingman R, Balu-Iyer SV. Immunogenicity of protein pharmaceuticals. *J Pharm Sci*. 2018;108(5):1637-1654.
19. Keizer RJ, Huitema ADR, Schellens JHM, Beijnen JH. Clinical pharmacokinetics of therapeutic monoclonal antibodies. *Clin Pharmacokinet*. 2010;49(8):493-507.
20. Louizos C, Yáñez JA, Forrest ML, Davies NM. Understanding the hysteresis loop conundrum in pharmacokinetic /pharmacodynamic relationships. *J Pharm Pharm Sci*. 2014;17(1):34-91.
21. Hernando N, Wagner CA. Comprehensive physiology. *Compr Physiol*. 2018;8(3):1065-1090.
22. Mehrotra N, Bhattaram A, Earp JC, et al. Role of quantitative clinical pharmacology in pediatric approval and labeling. *Drug Metab Dispos*. 2016;44(7):924-933.

Supplemental Information

Additional supplemental information can be found by clicking the Supplements link in the PDF toolbar or the Supplemental Information section at the end of web-based version of this article.